5th ECPMG Delft · 2024

Proceedings of the 5th ECPMG 2024
5th European Conference on Physical Modelling in Geotechnics
2-4 October 2024, Delft, the Netherlands

Development of an apparatus for physical modeling of tailings dams: preliminary tests

A. H. Rocha, *antonio.hilario@coc.ufrj.br,* M. S. S. Almeida, *almeida@coc.ufrj.br*,
COPPE - Universidade Federal do Rio de Janeiro, Brasil.

L. D. B. Becker, *leonardobecker@poli.ufrj.br*, M. C. F. Almeida, *mariacascao@poli.ufrj.br,*
POLI - Universidade Federal do Rio de Janeiro, Brasil.

J. R. M. S. Oliveira, *jrmso70@gmail.com*, W. L. Oliveira Filho, *wlofilho@gmail.com*
COPPE - Universidade Federal do Rio de Janeiro, Brasil.

F. A. M. Guerra, *fguerrageotec@gmail.com*
VALE, Minas Gerais, Brasil.

ABSTRACT: Recent environmental disasters resulting from mine tailings dam failures, with significant loss of life and widespread impact, have prompted public response and more stringent regulatory measures. These structures, mostly composed of sand and silt particles with high water content and low density, can be susceptible to liquefaction. The use of physical models in geotechnical engineering has proven to be crucial, allowing controlled simulations of complex systems and providing essential insight into the understanding of dam stability. This paper presents the development of a test apparatus for the evaluation of scaled models of iron ore tailings dams. This allows different types of tailings structures to be simulated and can be used as benchmark for numerical analysis. Preliminary tests are presented to validate the capabilities of the apparatus. The methodology includes characterization of geotechnical parameters, flow analysis, and stability assessment. The paper presents the results of preliminary tests aiming to a better understanding of the geotechnical behavior of tailings, which is essential for improving dam design, construction and management practices to reduce the risks associated with environmental disasters.

1 INTRODUCTION

Accidents related to static liquefaction in tailings dams have been reported in the literature in recent years (Morgenstern et al., 2016; Robertson et al., 2019; Jefferies et al, 2019), prompting a number of experimental and numerical studies on the topic (e.g., Becker et al., 2023; Whittle et al., 2022).

To understand the flow behavior and stability of tailings dams, a large-scale apparatus has been developed in partnership with the global mining VALE company. This paper presents preliminary simulations of physical models using this test apparatus, complemented by flow and stability analyses. The validation of the operating assumptions of the test box presented here will allow this equipment to be used in future research involving simulation of static liquefaction in tailings dams.

2 MATERIALS AND METHODS

2.1 Tailings soil studied

The tailings used in this study are typical of materials found in tailings dams in the Iron Quadrangle in the state of Minas Gerais, Brazil. In the specific dam where the soil was collected, the underflow and overflow materials have similar grain size curves. The overflow material was chosen for this experimental study because the critical failure circles in the stability analysis of the dam cross predominantly this material. Piezocone tests performed on the dam yielded a typical relative density of 30% and a zero-state parameter, indicating a contractive soil, therefore susceptible to liquefaction (Jefferies and Been, 2016).

2.2 Geotechnical parameters of the tailings

The grain size distribution of the collected material is shown in Figure 1, together with the tailings considered representative of the material contained in the Córrego do Feijão dam (Viana da Fonseca et al., 2022). The tailings from this study consist of fine silty sand, composed of 52% sand, 46% silt and 2% clay, with D_{50} = 0.06 mm and a coefficient of uniformity equal to 2, classified as well-graded, in addition to being non-plastic. The specific gravity of the particles, G_s, is equal to 2.93, compatible with the range of

values reported by Carneiro et al. (2023) for mining tailings from the Iron Quadrangle.

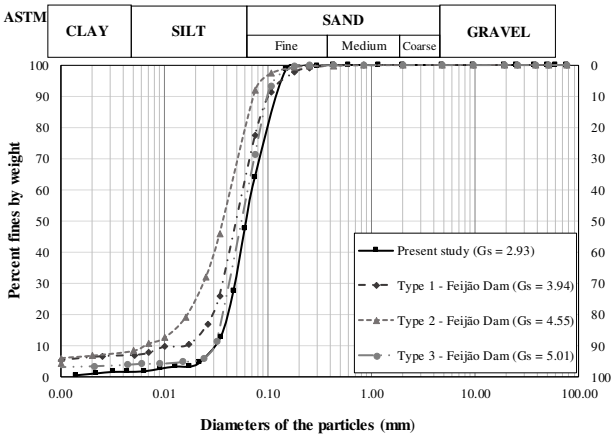

Figure 1 - Comparison of the particle size distribution of the tailings under study and the tailings from the B1 dams at Córrego do Feijão and Fundão.

To achieve better compatibility between the 1g physical model and the real structure idealized as a prototype, the same state parameter (Jefferies and Been, 2016) measured in the prototype was used in the physical model. The state parameter ψ is defined as the difference between the in-situ void ratio e and the critical state void ratio e_c for the same value of mean effective stress p', so $\psi = e - e_c$, assuming $\psi = 0$, $e = e_c$.

A campaign of drained and undrained triaxial tests (Coutinho, 2022) determined the critical state line for the tailings, and Equation 1 was obtained.

$$e_c = 0.97 - 0.030\ln(p') \quad (1)$$

The reference p'-value in the prototype is approximately 800 kPa, while in the model it is much lower, specifically p'= 5.5 kPa. Therefore, the void ratio in the model must be higher than in the prototype. By substituting these values for p', void ratios of 0.77 and 0.92 are obtained for the prototype and model, respectively.

Constant head permeability tests on compacted specimens with a nominal void ratio of 0.92 yielded an average vertical permeability coefficient $k_v = 8.8 \cdot 10^{-6}$ m/s. The permeability tests in the horizontal direction indicated that the compacted soil was nearly isotropic.

2.3 Test apparatus used for physical modeling and instrumentation

The metal box used in the physical models, shown in Figure 2, is 4.3 m long, 1.0 m high, and 1.0 m wide, with 5 acrylic panels on each side. A schematic drawing of the box in elevation and plan, showing the drainage system and reservoir, is shown in Figure 2a and Figure 2b, respectively. The evaluation of models with varying slope angles and pore pressure conditions may be used for the comparison and validation of different numerical simulations.

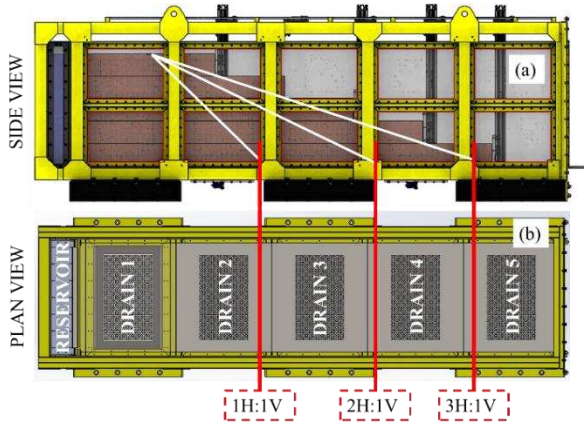

Figure 2 - (a) Schematic drawing to define the geometries of the research; (b) Drainage system and reservoir

The box has a reservoir at one end to control the water level using pumps and piezometric sensors. The drainage at the bottom can be controlled by allowing a free or blocked flow.

Figure 2 also shows a schematic representation of the three slopes analyzed by Rocha Junior (2023). Due to page limitations, more emphasis is given on the results of the 1V:1H slope tests. In the present paper, the results of the model slope 1V:2H are to the evaluation of the behavior of the optical fiber inclinometer. It should be noted that the final slopes tested are continuous, without the "steps" shown in Figure 2, which represent the situation of the dam after compaction.

Electric piezometers were used to monitor the water flow in the dam. They were 0.162 m long and 0.026 m in diameter, with a bronze filter, a 20 kPa scale, and a resolution of 0.005 kPa. Figure 3 shows 2 piezometers installed at the base of the box and also shows the non-woven geotextile placed over the drainage system. The green structure in the same figure is the base of one of the optical inclinometers.

Figure 3 - Installation of piezometers and base of optical inclinometer

The optical inclinometer was constructed using a thin acrylic rod, 1 m long, 0.015 m wide and 0.003 m thick, and two strands of single-mode optical fiber, each containing 5 fiber Bragg gratings (FBGs). The strands were bonded to opposite sides of the rod using a cyanoacrylate-based adhesive. The FBGs were inscribed into the strands 0.2 m apart.

A FBG is a periodic modulation in the refractive index of the optical fiber core resulting from exposure to an ultraviolet radiation interference pattern (Werneck et al., 2017).

Figure 4 illustrates the working principle of a FBG. A small portion of the incident light spectrum is reflected, with the central wavelength of the reflected light referred to as the Bragg wavelength. This value varies according to temperature and strain.

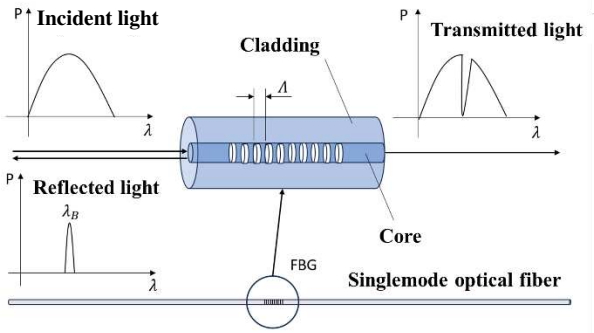

Figure 4 - Operating principle of a fiber Bragg grating

The wavelength variation readings were obtained using a model SI155 interrogator from the manufacturer Luna Micron Optics, with a wavelength accuracy of 1 picometer.

The strain values measured by the FBGs were converted to soil displacement using the conjugate beam method according to Zheng et al. 2019, in which the FBGs are considered in a differential configuration to compensate for temperature effects.

The inclinometer was calibrated using a system consisting of a linear guide and a laser displacement sensor (LDS) as a reference instrument. This system was mounted on an optical table where the inclinometer was subjected to predefined curvatures. In the bench tests, the inclinometer showed an approximate resolution of 0.0001 m, repeatability of 0.0008 m, absolute errors of less than 0.004 m for the evaluated measurement range of up to 0.050 m (Oliveira Filho, 2023).

The optical inclinometer (displacement sensor) was installed, as shown in Figure 5, on the physical model 1V:2H. It is noted that PZ3 was not used in model 1V:1H.

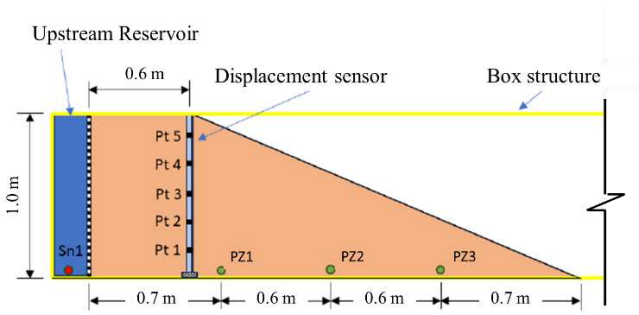

Figure 5 - Schematic drawing of instrumentation – model 1V:2H

2.4 Tailings soil compaction in the model

The soil in the model was compacted using a custom-built semi-automatic device whose main components are a weight, an impact plate and vertical guides (Figure 6). The compaction equipment is mounted on a frame to facilitate its movement throughout the box.

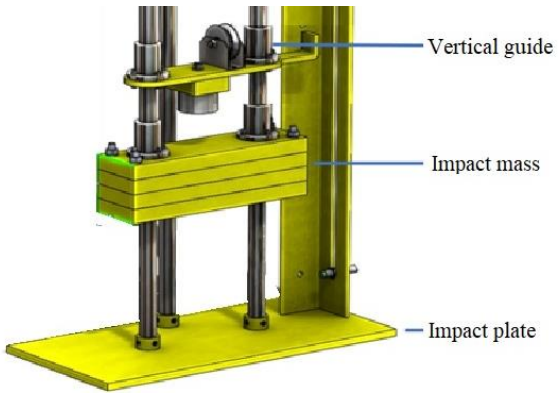

Figure 6 - Semi-automatic compaction equipment

The physical models, as well as the specimens used in the triaxial tests, were prepared using the Modified Moisture Tamping (MMT) technique developed by Bradshaw and Baxter (2007), which is a variation of the Moisture Tamping (MT) technique (Ladd, 1978). The MMT technique ensures consistent density throughout the height of the sample by varying the energy during the compaction process. Prior compaction tests are necessary to determine the drop height for each layer.

In order to compact a model with a slope, barriers were used to retain the soil as shown in Figure 7.

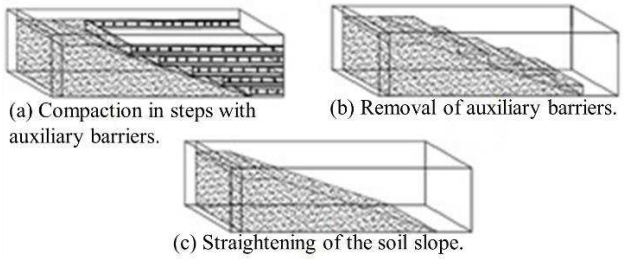

Figure 7 – Slope model compaction process.

Figure 8 shows the 1(V):1(H) model immediately after removing the barriers (a) and after trimming (b).

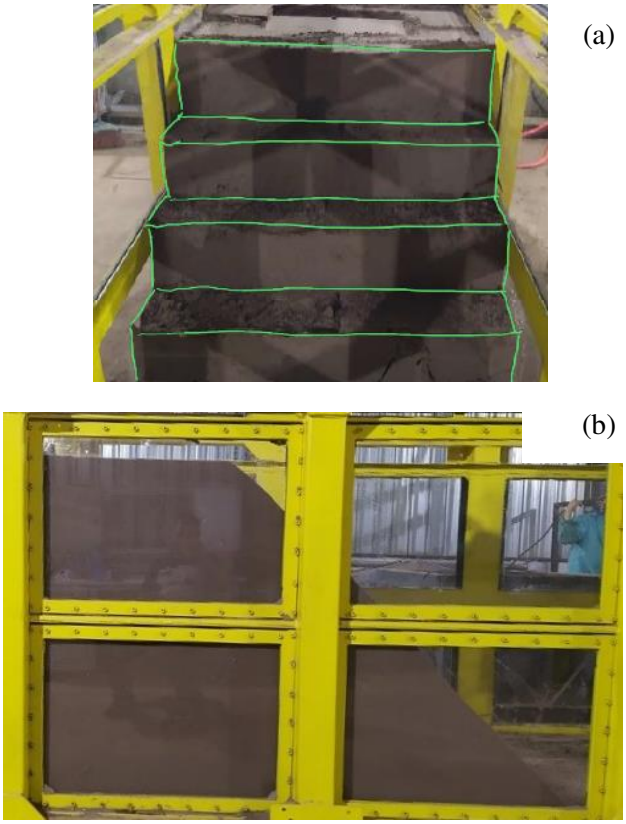

Figure 8 – (a) Immediately after removing the auxiliary blocks; (b) After trimming (final geometry)

Table 1 shows the model construction data. The void ratio obtained was slightly higher than the target void ratio of 0.92.

Table 1 - Construction data for the 1V:1H model

Model Volume (m^3)	Mass (kg)	Water Content (%)	$\rho_n(\frac{g}{cm^3})$	e_0	ψ
1.10	1810	10.5	1.65	0.96	0.04

3 RESULTS

3.1 Model with slope 1V:1H

The purpose of this paper is to demonstrate the capabilities of the test apparatus and to evaluate the functionality of the systems. A slope inclination of 1V:1H was adopted for the first test due to its smaller size and to ensure failure. Two piezometers were placed at the base of the model (PZ1, PZ2, Figure 9a). Initially, the reservoir water level was set to 0.70 m until the readings from the piezometers stabilized, and then set to zero for the start of the test. The reservoir water level was then increased to 0.95 m, increasing the measured pore pressure shown in Figure 9b.

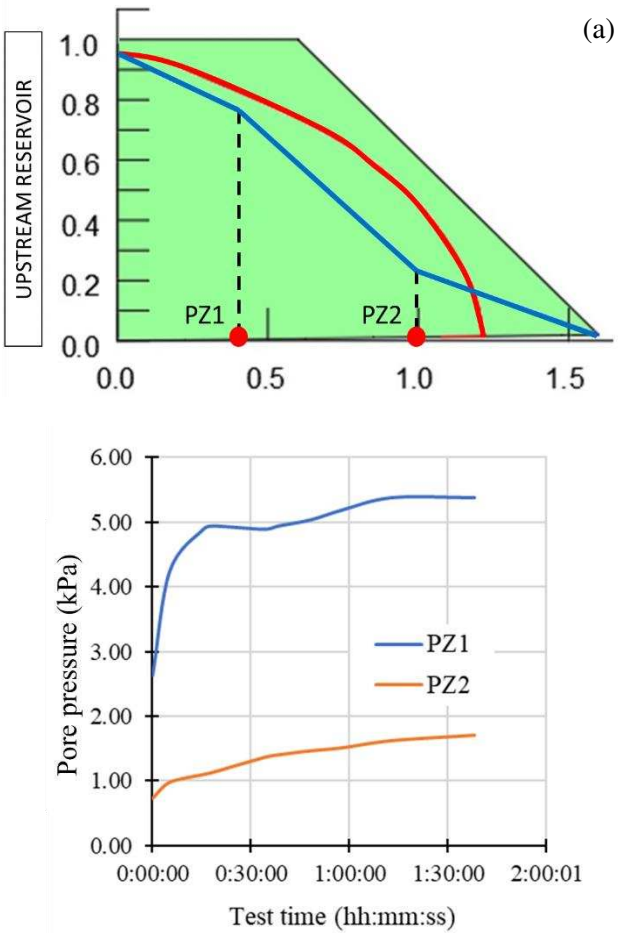

Figure 9 - (a) Phreatic line of the flow analysis (red line) and of the physical model (blue line) in stationary regime; (b) Piezometer data during transient flow

The water level in the model was estimated by measuring the pore pressure at the base. In later models, stand-pipe piezometers were installed in the acrylic wall to directly assess the water level.

Figure 9a shows that the phreatic line of the physical model (blue line) is slightly below the phreatic line of the flow analysis (red line). In contrast to the numerical prediction, the blue line intersects the toe of the slope likely because water created a concentrated flow path close to the corners between the base and the walls of the test box. In other words, the measured pore pressures were lower than those predicted by the flow analysis. The difference between the phreatic line in the numerical model and the physical model can be explained by the lack of complete watertightness at the base of the test box, which affected the flow network. Leakage problems in the test box were later eliminated.

The stability analysis also required identifying the beginning of slope failure relative to the slope crest, as

depicted in Figure 10. This distance was used in the stability analysis to limit the entry zone of the search for the critical surface. The aim was to obtain a slip surface in the stability analysis that is similar to the failure surface identified visually during the test.

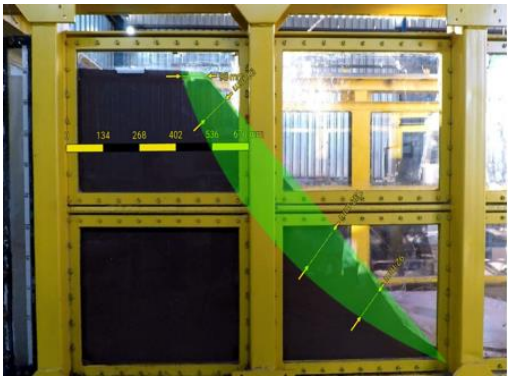

Figure 10 - Distance between the slope crest and the slip surface

Figure 11 displays the stability analysis for the 1V:1H model based on numerical flow analysis, with the slip surface depicted in white and a safety factor FS = 1.0. The limit equilibrium analysis was chosen to assess whether the test conditions were capable of inducing a state of imminent failure of the model. In the future, finite element analysis will be performed for comparison with the displacement measurements. The material was assigned the following properties: unit weight of 19.5 kN/m³, friction angle of 34.8°, and zero effective cohesion (Coutinho, 2022). Liquefaction did not occur in this test as the failure surface was located in an unsaturated region of the physical model. Figure 11 illustrates that only a small portion of the failed tailings mass was beneath the water level.

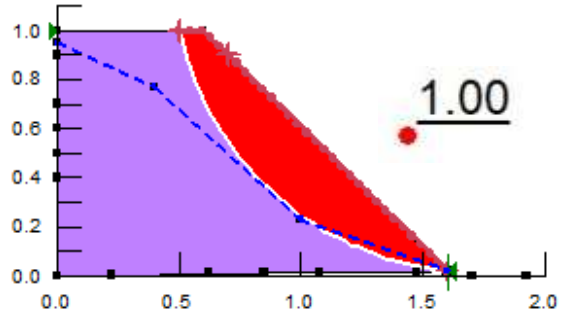

Figure 11 - Stability analysis using the flow network obtained from the physical model.

3.2 Model with slope 1V:2H

In a second test, a 1V:2H slope inclination was used. This model failed after a surcharge load was applied to its crest. Profiles of horizontal displacements of the model obtained using the optical inclinometer are shown in Figure 12. Three displacement profiles are shown, representing different moments: the last measurement before loading (395 minutes), seconds after loading (405 minutes), and 70 minutes after loading (475 minutes - failure propagation). Pre-loading displacements (before 395 minutes) were associated with the rise in water level. After loading, the displacements increased sharply. Based on the rotation measured in the inclinometer at the onset of failure, a failure mechanism similar to the general shear of a shallow foundation was inferred.

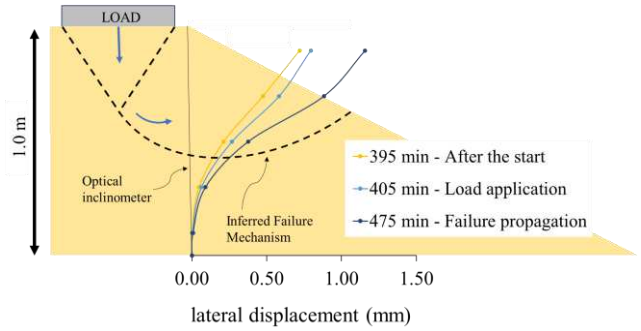

Figure 12 – Profiles of horizontal displacements

Figure 13 presents the distortion rate variations over time for the central region of the model (Oliveira and Almeida, 2001; Almeida and Marques, 2013). The distortion angle (expressed in %) is defined as the arctangent of the ratio between the difference of two consecutive horizontal readings and the difference in their corresponding depths. According to the authors, the distortion rates, which are the variation of the distortion angles over time (expressed in %/day), should be below 0.5%/day for stable embankments and above 1.5%/day for unstable embankments in a failure process. For distortion rates between 0.5 and 1.5%/day caution is advised.

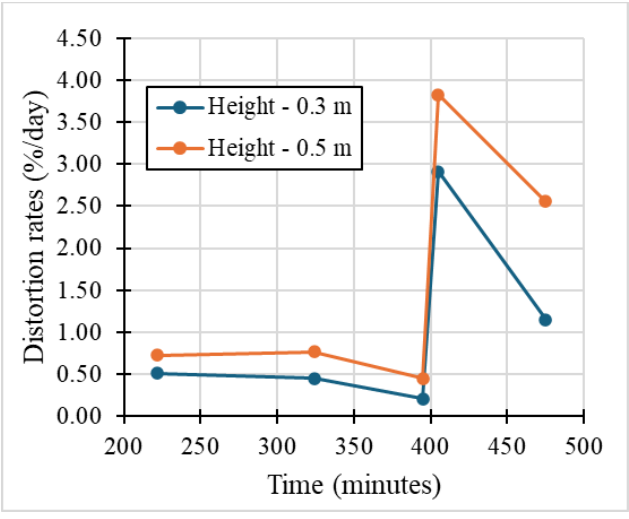

Figure 13 - Distortion rates x time.

Concerning the rates at 0.5 m model height, where the highest distortions were observed, the values were found to be approximately 0.73%/day and 0.77%/day during the phreatic line increase (times 222 minutes and 324 minutes), and 0.45%/day after phreatic stabilization and before load application (time 395 minutes). Following the loading event (time 405 minutes), the distortion rate increased to 3.83%/day, indicating a failure. Even at 475 minutes, the values remained around 2.56%/day.

4 CONCLUSIONS

The measured pore pressures and horizontal displacements validated the flow analysis and slope stability analysis, demonstrating the capability of the apparatus to physically simulate tailings structures.

The stability analysis also demonstrated consistency with the failure surface observed in the model. The consistent horizontal displacements measured by the fiber optical inclinometer suggest that this type of instrument has a significant potential for use in physical models.

ACKNOWLEDGMENTS

The authors would like to thank VALE SA for the financial support to the development of this research and also CAPES and CNPq for providing the scholarships.

REFERENCES

Almeida, M. S. S. and Marques, M.E.S. (2013). “Design and Performance of Embankments on Very Soft Soils.”, 1. ed. CRC Press - Taylor & Francis Group.

Becker LDB, Ehrlich M, Barbosa MC (2023), “Discussion of stability analysis of upstream tailings dam using numerical limit analyses.” https://doi.org/10.1061/JGGEFK.GTENG-11272

Bradshaw, A. S., and C. D. Baxter (2007). "Sample preparation of silts for liquefaction testing." Geotechnical Testing Journal 30, 4: 324-332. https://digitalcommons.uri.edu/cve_facpubs/118

Carneiro, J.J.V., Marques, E.A.G., Viana da Fonseca, A.J.P. et al. (2023). “Characterization of an Iron Ore Tailing Sample and the Evaluation of Its Representativeness.” Geotech Geol Eng 41, 2833–2852. https://doi.org/10.1007/s10706-023-02430-8

Coutinho, R. S. (2022), “Experimental Studies and Norsand Model Applied to an Iron Ore Tailings. (in portuguese)”, MSc Thesis, Universidade Federal do Rio de Janeiro, COPPE, Programa de Engenharia Civil, Rio de Janeiro.

Geo-Slope International Ltd (2021), SEEP/W Tutorial – Getting Started, GEO-SLOPE International Ltd., Calgary, Alberta, Canada.

Geo-Slope International Ltd (2021), SLOPE/W User Manual, GEO-SLOPE International Ltd., Calgary, Alberta, Canada.

Jefferies, M. G., K. Been. (2016). “Soil Liquefaction – A Critical State Approach”, 2nd ed. London: Taylor and Francis.

Jefferies, Morgenstern, NR Van Zyl, D Wates, J. (2019), “Report on NTSF Embankment Failure” Cadia Valley Operations for Ashurst Australia.

Ladd, R. S. (1978), “Preparing Test Specimen using Undercompaction,” Geotechnical Testing Journal, Vol. 1, No. 1, pp. 16-23. http://dx.doi.org/10.1520/GTJ10364J

Morgenstern NR, Vick SG, Viotti CB, Watts BD (2016), Fundão Tailings Dam Review Panel–Report on the Immediate Causes of the Failure of the Fundão Dam. The Fundão Tailings Dam Investigation, Belo Horizonte, MG, Brazil.

Oliveira Filho, W. L. (2023), “Fbg-based Soil Displacement Sensor for Application in a Physical Model of a Mining Tailings Dam. (in portuguese)”, MSc Thesis, Universidade Federal do Rio de Janeiro, COPPE, Electrical Engineering Program, Rio de Janeiro.

Oliveira JRMS and Almeida MSS (2001). “Stability control of embankments built on soft clays.” In: 3rd International Conference on Soft Soil Engineering, Hong Kong. Soft Soil Engineering. Lisse: A.A. Balkema Publishers, p. 435-440.

Robertson PK, De Melo L, Williams DJ, Wilson GW (2019), “Report of the expert panel on the technical causes of the failure of Feijão Dam I, Brazil”.

Rocha Junior A. (2023), “Study of Static Liquefaction for Tailings Dams in 1G Modeling. (in Portuguese)”, MSc Thesis, Universidade Federal do Rio de Janeiro, COPPE, Civil Engineering Program, Rio de Janeiro.

Viana da Fonseca, A., Cordeiro, D., Molina-Gómez, F., Besenzon, D., Fonseca, A., e Ferreira, C. (2022), “The mechanics of iron tailings from laboratory tests on reconstituted samples collected in post-mortem Dam I in Brumadinho.”, Soils and Rocks, 45(2). https://doi.org/10.28927/SR.2022.001122

Werneck, M. M. M., Allil, R. C., De Nazaré, F. V. Fiber (2017), “Bragg Gratings: Theory, Fabrication, and Applications”, v. TT 114, Tutorial texts in optical. Bellingham, Washington, SPIE.

Whittle, A. J., et al. (2022), “Stability Analysis of Upstream Tailings Dam Using Numerical Limit Analyses”, Journal of Geotechnical and Geoenvironmental Engineering, v. 148. https://doi.org/10.1061/(ASCE)GT.1943-5606.0002792

Zheng, Y., Zhu, Z. W., Deng, Q. X., et al. (2019), “Theoretical and experimental study on the fiber Bragg grating-based inclinometer for slope displacement monitoring”, Optical Fiber Technology, v. 49, n. October 2018, pp. 28–36. https://doi.org/10.1016/j.yofte.2019.01.031